

# Analytical estimates of proton acceleration in laser-produced turbulent plasmas

Konstantin Beyer,<sup>1,\*</sup> Brian Reville,<sup>2</sup> Archie Bott,<sup>1</sup> Hye-Sook Park,<sup>3</sup> Subir Sarkar,<sup>1,4</sup> and Gianluca Gregori<sup>1</sup>

<sup>1</sup>*Department of Physics, University of Oxford, Parks Road, Oxford OX1 3PU, UK*

<sup>2</sup>*School of Mathematics and Physics, Queens University Belfast, Belfast BT7 1NN, UK*

<sup>3</sup>*Lawrence Livermore National Laboratory, P.O. Box 808, Livermore, California 94551, USA*

<sup>4</sup>*Niels Bohr Institute, Blegdamsvej 17, 2100 Copenhagen, Denmark*

(Dated: December 14, 2024)

With the advent of high power lasers, new opportunities have opened up for simulating astrophysical processes in the laboratory. We show that 2nd-order Fermi acceleration can be directly investigated at the National Ignition Facility, Livermore. This requires measuring the momentum-space diffusion of 3 MeV protons produced within a turbulent plasma generated by a laser. Treating Fermi acceleration as a biased diffusion process, we show analytically that a measurable broadening of the initial proton distribution is then expected for particles exiting the plasma.

## I. INTRODUCTION

Turbulent magnetic fields are ubiquitous in the universe and their role in determining energetic particle transport is key to understanding the confinement and acceleration of high-energy cosmic rays [1–5]. As particles traverse a turbulent, magnetised plasma, they undergo a random walk in both physical and momentum space. The latter process is referred to as 2nd-order Fermi acceleration, being a generalization of the mechanism proposed by Fermi [6]. Fermi observed that repeated elastic scattering of fast particles off slow moving ‘magnetised clouds’, when averaged over a random distribution of cloud velocities produce a net gain in energy. The rate of energy gain is slightly higher than the rate of energy loss because head-on collisions are more probable than overtaking ones, the net gain being proportional to  $(u/v)^2$  where  $u$  is the mean fluid velocity and  $v(\gg u)$  the particle velocity. Subsequently the focus has shifted from discrete interactions with magnetised clouds to continuous scattering in magneto-hydrodynamic (MHD) turbulence, but the underlying principle remains the same. Fermi noted shortly afterwards that converging flows such as might exist between Galactic spiral arms result in a faster 1st-order process where the energy gain is proportional to  $u/v$  [7]. Indeed 1st-order Fermi acceleration in the converging fluid flow at astrophysical shock waves is currently the preferred model for the origin of cosmic rays [8–10]. However the 2nd-order mechanism can be more efficient for accelerating non-relativistic thermal background plasma particles and under certain conditions can also preferentially accelerate electrons relative to protons as is required to explain many astrophysical sources [11]. In reality there may be a hybrid mechanism, e.g. initial 2nd-order acceleration of background plasma particles by turbulence, followed by a second stage of 1st-order acceleration by a shock wave.

The 2nd-order Fermi process is quite general, requiring only turbulent magnetised fluid motions and injection

of particles with energy above that of the background thermal plasma. Relevant environments are common in the universe and stochastic acceleration is believed to be responsible for phenomena as diverse as e.g. radio emission from young supernova remnants entering the Sedov-Taylor phase [12], the ejection of mass from the Solar corona [13], the acceleration of particles in the jets of active galactic nuclei and in their giant radio lobes [14–16] and  $\gamma$ -ray emission from the Fermi bubbles [17].

The necessary conditions may be accessible in laboratory experiments [5] thus providing a platform to explore particle acceleration in a controlled setting and isolate effects of relevance to astrophysical models. We explore here the possibility of validating the physics of 2nd-order Fermi acceleration using existing experimental set-ups (see supplementary material to Ref.[18]). In § II we introduce the proposed set-up and place it in the context of previous experiments. The governing equations for the momentum space diffusion process are stated in § III and the relevant Fokker-Planck coefficients of the diffusion process are estimated. We discuss the relevant time scales to justify the diffusion approach adopted. An analytic solution for the diffusion equation is investigated in § IV. Finally in § V, laser experiments at the National Ignition Facility (NIF), Livermore, USA [19] are discussed. We conclude that the effects of stochastic Fermi acceleration are measurable in the laboratory.

## II. EXPERIMENTAL SET-UP

Experiments with high power lasers have achieved conditions where strong magnetised turbulence can be sustained over large spatial scales and thus provide insights on the origin and amplification of magnetic fields in the intergalactic medium [5, 18, 20, 21]. Tzeferacos et al. [18] describe how a high power laser was used to generate two counter streaming plasma flows from direct ablation of CH (plastic) foils. Each flow was guided through a grid of  $300\ \mu\text{m}$  holes with  $300\ \mu\text{m}$  spacing between holes. The grids were spatially shifted to increase turbulent motions in the plasma and enhance the turbulent dynamo

\* Correspondence to konstantin.beyer@physics.ox.ac.uk

RMS magnetic field	$B \sim 1.2 \text{ MG}$
mean turbulent velocity	$u = 0.002c$
scale of the turbulence cells	$\ell \sim 0.06 \text{ cm}$
plasma size	$L = 0.4 \text{ cm}$
initial proton momentum	$p_0 = 0.002 m_p c$
density relation	$\nabla n/n \sim \mathcal{O}(1)$
temperature	$T = 700 \text{ eV}$

TABLE I: The expected plasma parameters for the proposed experiment at the NIF, LLNL. These are derived from experiments done at other facilities [18], rescaled to NIF laser drive conditions.

processes responsible for amplification of magnetic seed fields. This produced turbulent structures with an outer scale of  $\sim 600 \mu\text{m}$  in the colliding region. These results were obtained using multi-kJ laser systems. At the NIF, a MJ of laser energy is available so more extreme conditions are to be expected as shown in Table I.

We adopt these estimated parameters in order to assess the feasibility of a ‘cosmic ray acceleration platform’ in the laboratory. The first step is the injection of cosmic ray particles, which can be implemented by replacing the CH foils used earlier [18] by CD (deuterated plastic) foils. Within the turbulent plasma region, 3 MeV protons (with velocity  $v_p \sim 8 \times 10^{-2} c$ ) will be produced via D-D collisions in the counter-streaming plasma flows [22]. Analogous to the astrophysical situation, these protons as they stream out from the plasma interact with the turbulent magnetic fields and should be accelerated by the 2nd-order Fermi process. We now model this interaction to predict the energy spectrum of the protons.

As each scatter changes the energy of a particle by a small fraction of its initial energy, this is a diffusion process in momentum space described by a Fokker-Planck transport equation for  $f(p, t)$ , the phase space density of the protons in the plasma [1, 10, 23, 24]:

$$\left( \frac{\partial f}{\partial t} \right)_{\text{inner}} = \frac{1}{p^2} \frac{\partial}{\partial p} \left( p^2 D_p \frac{\partial f}{\partial p} \right) - \frac{f}{\tau_{\text{esc}}} + \frac{C_0 \delta(p - p_0) \delta(t - t_0)}{4\pi p^2}. \quad (1)$$

Here  $D_p$  is the momentum diffusion coefficient,  $\tau_{\text{esc}}$  the escape time describing the loss of protons from the system and the last term describes instantaneous injection ( $C_0$ ) of superthermal particles at time  $t_0$  and momentum  $p_0$ . Note that spatial homogeneity is assumed in writing down Eq. (1), however we will assume that the injection occurs only in the central region of the plasma. The particle distribution function  $n$  is related to the phase space density  $f$  through

$$n(p, t) = 4\pi p^2 f(p, t). \quad (2)$$

The diffusion equation (2) has been solved for a variety of situations [1, 12, 23, 25, 26] and we discuss below the appropriate solution for the proposed experiment.

The detectors used to measure the proton energy are located outside the plasma, hence the relevant distribution function to consider is that of the *escaping* protons. This can be related to the particle distribution function of the protons inside the plasma by requiring that proton number be conserved after the injection, i.e. at  $t > t_0$

$$\left( \frac{\partial n}{\partial t} \right)_{\text{outer}} = \frac{n_{\text{inner}}}{\tau_{\text{esc}}}, \quad (3)$$

where  $f_{\text{inner}}$  is the solution of Eq.(1). As will be shown in §III, the escape time  $\tau_{\text{esc}}$  is momentum-dependent so the phase space density inside and outside the plasma will be *different*.

### III. THE TRANSPORT COEFFICIENTS

The Fokker-Planck transport coefficient for energy diffusion is [e.g. 10]

$$D_\epsilon = \frac{\langle (\Delta\epsilon)^2 \rangle}{\Delta t}, \quad (4)$$

where  $\langle \cdot \rangle$  denotes the average over scattering angles, and the energy change per scatter is given by the integral over the force exerted by the electric field fluctuations, i.e.

$$\langle (\Delta\epsilon)^2 \rangle = \left\langle \left( e \int \mathbf{E} \cdot d\mathbf{s} \right)^2 \right\rangle \sim e^2 \ell^2 \langle (E_{||})^2 \rangle. \quad (5)$$

Here,  $\mathbf{s}$  is the world-line of the particle and  $\ell$  is the scale length of the turbulence cells in the plasma flow. These cells are defined by the scale on which the electric field,  $\mathbf{E}$ , is statistically de-correlated, close to the outer scale of the turbulent spectrum.

The appropriate Ohm’s law reads [27]:

$$\mathbf{E} = -\frac{\mathbf{u} \times \mathbf{B}}{c} - \frac{\nabla P_e}{ne}, \quad (6)$$

where  $P_e$  is the isotropic electron pressure,  $n$  is the electron density and  $\mathbf{u}$  is the electron velocity field. In principle Ohm’s law contains possible additional contributions but these turn out to be small in the present case as e.g. the Reynolds and magnetic Reynolds numbers are large.

Note that for the assumed conditions at the NIF (Table I), the pressure term is insignificant, being of  $\mathcal{O}(10^{-2})$ . We will retain it nevertheless as it is relevant for conditions achievable at other facilities such as OMEGA [28].

Returning to the Fokker-Planck transport coefficient (4), we find by combining Eqs.(5) and (6)

$$\begin{aligned} \langle (\Delta\epsilon)^2 \rangle = & e^2 \ell^2 \left\langle \left( \frac{u^2 B^2}{c^2} \sin^2(\theta) \right) \right\rangle + e^2 \ell^2 \left\langle \left( \frac{\nabla P_e}{ne} \right)^2 \right\rangle \\ & + 2e^2 \ell^2 \left\langle \left( \frac{uB}{c} \left| \frac{\nabla P_e}{ne} \right| \sin(\theta) \cos(\phi) \right) \right\rangle, \end{aligned} \quad (7)$$

with  $\theta$  the angle between  $\mathbf{u}$  and  $\mathbf{B}$  and  $\phi$  the angle for the inner product of the two terms in (6) after squaring.

Treating the electrons as an ideal gas, one finds for the electron pressure term:  $\nabla P_e = e\nabla(nT)$ . Due to the large electron thermal conduction, the temperature remains approximately constant across the plasma [18], hence pressure fluctuations are due only to density variations. This also implies that the angles  $\theta$  and  $\phi$  are uncorrelated, hence the averaging gives

$$\langle(\Delta\epsilon)^2\rangle = \ell^2 \left[ \frac{4e^2}{3c^2} u^2 B^2 + e^2 T^2 \left( \frac{\nabla n}{n} \right)^2 \right]. \quad (8)$$

The relevant time scale for this energy change depends on the parameters of the system. This can be in one of two regimes — ballistic escape or true diffusion — according to how the pitch angle scattering time compares to the time a proton needs to escape the plasma.

The relevant time scale determining the Fokker-Planck coefficient (4) is the time it takes a proton to cross a turbulent cell, taken to be of the order of the grid size i.e.,  $\Delta t \sim \ell/v_p$ . For the magnetic field values expected in the NIF experiment (Table I), the proton gyro-radius is  $r_g \sim 0.2$  cm, i.e. larger than the turbulent cell scale, so particles are *unmagnetised*. Hence proton propagation can be described as a random walk until escape from the plasma. Since the protons are non-relativistic, we have

$$\Delta t \sim \frac{\ell}{v_p} = \frac{m_p \ell}{p}, \quad (9)$$

where  $p = m_p v_p$  is the proton momentum.

Moreover in this case,  $(\Delta\epsilon)^2 = (p^2/m_p^2)(\Delta p)^2$ , so the momentum diffusion coefficient is from Eqs.(8) and (9):

$$D_p = \frac{\langle(\Delta p)^2\rangle}{\Delta t} \sim \frac{\ell}{c} \left[ \frac{4e^2 B^2}{3} \frac{u^2}{c^2} + e^2 T^2 \left( \frac{\nabla n}{n} \right)^2 \right] \frac{m_p c}{p}. \quad (10)$$

We note the dependence  $D_p \propto p^{-1}$ . In the traditional moving cloud picture, diffusion is *less* efficient for particles with higher momentum because the difference in probability for head-on and over-taking collisions is then smaller. In the present setup with MHD turbulence, particle trajectories are simply aligned with the electric field for a shorter time, provided they remain non-relativistic.

Next we need the spatial diffusion coefficient in order to determine the diffusive escape-time scale. The mean free path is the distance a proton travels before it is deflected by an angle  $\pi/2$  in a time  $\tau_{90}$  i.e.  $\lambda = v_p \tau_{90}$ . This can be estimated by treating the change in angle by each turbulence cell as a random walk process so the time to be scattered  $\pi/2$  away from the initial direction is,

$$\tau_{90} \sim \frac{r_g}{\omega_g \ell} = \frac{m_p^2 c^3}{\ell e^2 B^2} \frac{p}{m_p c}, \quad (11)$$

where  $\omega_g$  is the cyclotron frequency. The spatial diffusion coefficient is thus:

$$D_x = \frac{\langle(\Delta x)^2\rangle}{\Delta t} \sim \frac{1}{3} \frac{\lambda^2}{\tau_{90}} = \frac{m_p^2 c^5}{3e^2 \ell B^2} \left( \frac{p}{m_p c} \right)^3. \quad (12)$$

The spatial and momentum diffusion coefficients are related through:

$$D_p D_x = \frac{m_p^2 c^4}{3e^2 B^2} \left[ \frac{4e^2 B^2}{3} \frac{u^2}{c^2} + e^2 T^2 \left( \frac{\nabla n}{n} \right)^2 \right] \left( \frac{p}{m_p c} \right)^2. \quad (13)$$

The escape time  $\tau_{\text{esc}}$  is the time it takes a particle to diffuse out of the turbulent region of size  $L$ :

$$\tau_{\text{esc}} = \frac{L^2}{D_x} = \frac{3e^2}{m_p^2 c^5} \ell L^2 B^2 \left( \frac{p}{m_p c} \right)^{-3}. \quad (14)$$

This shows that particles with higher momentum get lost more efficiently, as is expected, since such particles stream out of the plasma faster, in addition to having a longer mean free path. Consequently, the mean momentum of particles outside the plasma will be higher due to the biased escape of mostly fast particles. Moreover, slower particles remain inside the plasma longer, accounting for their stronger acceleration.

As noted before, the system can be in two different limits: true diffusion or ballistic escape. The regimes are characterised by comparing the intrinsic time-scales of the system. Using the parameters from Table I the angular scattering time as defined by Eq.(11) is

$$\tau_{90} \sim \frac{r_g}{\omega_g \ell} \sim 1.5 \times 10^{-10} \text{ s} \left( \frac{B}{1.2 \text{ MG}} \right)^{-2} \left( \frac{\ell}{0.1 \text{ cm}} \right)^{-1}, \quad (15)$$

while the time needed to diffuse out of the plasma is:

$$\tau_{\text{esc}} = \frac{L^2}{D_x} \sim 5.5 \times 10^{-10} \text{ s} \left( \frac{B}{1.2 \text{ MG}} \right)^2 \left( \frac{\ell}{0.1 \text{ cm}} \right). \quad (16)$$

These must be compared with the time a proton would take to cross the plasma in the absence of magnetic fields:

$$t_{\text{cross}} = \frac{L}{v_p} = 1.7 \times 10^{-10} \text{ s}. \quad (17)$$

All the time scales above are of the same order, indicating that the conditions at NIF will be close to the transition from ballistic escape to the diffusive regime. We can optimistically also consider the case when  $B$  is larger by a factor of  $\sim 3$  (chosen to guarantee a factor  $\mathcal{O}(100)$  in the time-scales). Then  $B \sim 3.6$  MG and

$$\tau_{90} \sim 3.4 \times 10^{-11} \text{ s} < t_{\text{esc}} = 2.5 \times 10^{-9} \text{ s}. \quad (18)$$

It is now safe to assume true diffusion rather than ballistic escape.

#### IV. SOLVING THE DIFFUSION EQUATION

Given the diffusion and loss coefficients that we have derived, we can employ an analytical solution [26] obtained under the following assumptions. First, the initial and final proton distributions are assumed to be isotropic so the distribution function depends only on  $p = |\mathbf{p}|$ . In the present case, even if the turbulent plasma is produced by the collision of two counter propagating flows, their centre-of-mass is at rest, which suggests that the D-D proton emission is isotropic on average. However each individual D-D pair does not necessarily have a stationary centre-of-mass due to the temperature of the plasma jets so the initial energy distribution is not mono-energetic. We will discuss the implication of this in the next section. Experimental data show that the properties of turbulence are uniform within the interaction region of size  $L$  [18] so any spatial dependence may safely be neglected. Second, the plasma must be magnetised, which is the case for electrons in the proposed experiment (however, the ions are only weakly magnetised). Third, the proton energies must be relativistic. Although this is *not* the case here, the analytical solution [26] holds as long as  $D_p D_x \propto p^2$  and as shown earlier this relation remains valid even in the non-relativistic case.

Noting that  $D_p$  and  $\tau_{\text{esc}}$  are *constant* in time, the solution of Eq.(1), taking  $C_0 = 1$ , is [26] (see also [12, 25, 29, 30]):

$$n_{\text{inner}} = \frac{2\hat{p}^2\sqrt{\Psi}}{\sqrt{k\tau}(1-\Psi)} e^{-\frac{(\hat{p}^3+\hat{p}_0^3)(1+\Psi)}{3\sqrt{k\tau}(1-\Psi)}} I_0 \left[ \frac{4(\hat{p}\hat{p}_0)^{\frac{3}{2}}\sqrt{\Psi}}{3\sqrt{k\tau}(1-\Psi)} \right], \quad (19)$$

where  $\hat{p}$  and  $\hat{p}_0$  are dimensionless momenta, e.g.,  $\hat{p} = p/m_p c$ , and  $I_0$  is the modified Bessel function of the first kind. The function  $\Psi$  is defined as

$$\Psi(t, t_0) = \exp \left[ -6\sqrt{\frac{k}{\tau}}(t - t_0) \right], \quad (20)$$

with

$$k = \frac{D_p}{m_p^2 c^2} \frac{p}{m_p c}, \quad (21)$$

and,

$$\tau = \tau_{\text{esc}} \left( \frac{p}{m_p c} \right)^3. \quad (22)$$

In order to now determine the outer distribution function,  $n_{\text{outer}}$ , we can simply integrate Eq.(3) to find:

$$n_{\text{outer}}(p, p_0, t, t_0) = \int_0^t \frac{n_{\text{inner}}(p, p_0, t', t_0)}{\tau_{\text{esc}}} dt'. \quad (23)$$

Both distributions are shown in Fig. 1. Due to the scaling  $\tau_{\text{esc}} \propto p^{-3}$ , escape from the plasma is biased towards

higher momentum protons. This explains the decreasing mean momentum inside the plasma, since only the slower particles remain after a time comparable to  $\tau_{\text{esc}}$ . For the same reason the mean momentum outside the plasma is higher than on the inside. The momentum spectra shown in Fig. 1 were obtained by substituting the values for the plasma conditions given in Table I.

Momentum diffusion also changes the mean momentum of the proton distribution. We can obtain analytically the mean proton momentum *inside* the plasma:

$$\mu_{\text{inner}} = \frac{3^{1/3}}{\sqrt{k\tau}} \left[ k^2 \tau^2 \frac{(1-\Psi)^4}{(1+\Psi)^4} \right]^{1/3} \Gamma \left( \frac{4}{3} \right) \times \exp \left[ -\frac{4\Psi\hat{p}_0^3}{3\sqrt{k\tau}(1-\Psi^2)} \right] L_{-\frac{4}{3}} \left[ \frac{4\Psi\hat{p}_0^3}{3\sqrt{k\tau}(1-\Psi^2)} \right], \quad (24)$$

where  $L_{-\frac{4}{3}}$  are Laguerre polynomials, and  $\Gamma$  is the Gamma function. However the mean momentum outside can only be calculated numerically.

#### V. EXPERIMENTAL FEASIBILITY

The two relevant quantities that can be measured in a possible experiment are the shift in the mean energy and e.g. the full width at half maximum (FWHM) of the proton distribution. Of particular interest is the outer distribution, since that is where the detector is located. Given the available diagnostics, the measurement is essentially time-integrated, being the integral of Eq. (23) from the initial time to infinity.

In practice, it is sufficient to integrate up to a time late enough such that a significant portion of the protons have escaped from the plasma, indicated by the inner distribution dropping to near zero. A time of order  $10^3 \tau_{\text{esc}}$  proves sufficient as will be shown later. Also, the lower bound must be modified, due to the delta function nature of the distribution at  $t = t_0$ . Taking into account that the shortest time-scale on which a particle can exit the plasma is just crossing time, the lower bound on the integral can be chosen to be  $t_0 \sim \tau_{\text{esc}}$ . Then we obtain for the mean momentum of the escaping protons:

$$\mu_{\text{outer}} \sim \int_0^1 \hat{p} \int_{10^{-13}}^{10^{-7}} \frac{n_{\text{inner}}}{\tau_{\text{esc}}} dt d\hat{p} = 0.08 c, \quad (25)$$

which corresponds to a mean energy of 3.01 MeV. As expected, this is higher than at injection — by 10 keV which is  $\sim 3\%$  of the initial proton energy. The upper limit  $\hat{p} = 1$  was chosen to ensure that  $\hat{p} \gg \hat{p}_0$  and thus out of reach of the acceleration mechanism. This follows from the Hillas criterion [31], which provides an upper limit on the maximum energy gain by comparing the system size with the particle gyro-radius. The Hillas limit in our case is

$$E_{\text{Hillas}} = eBL \frac{u}{c} = 0.24 \text{ MeV}, \quad (26)$$

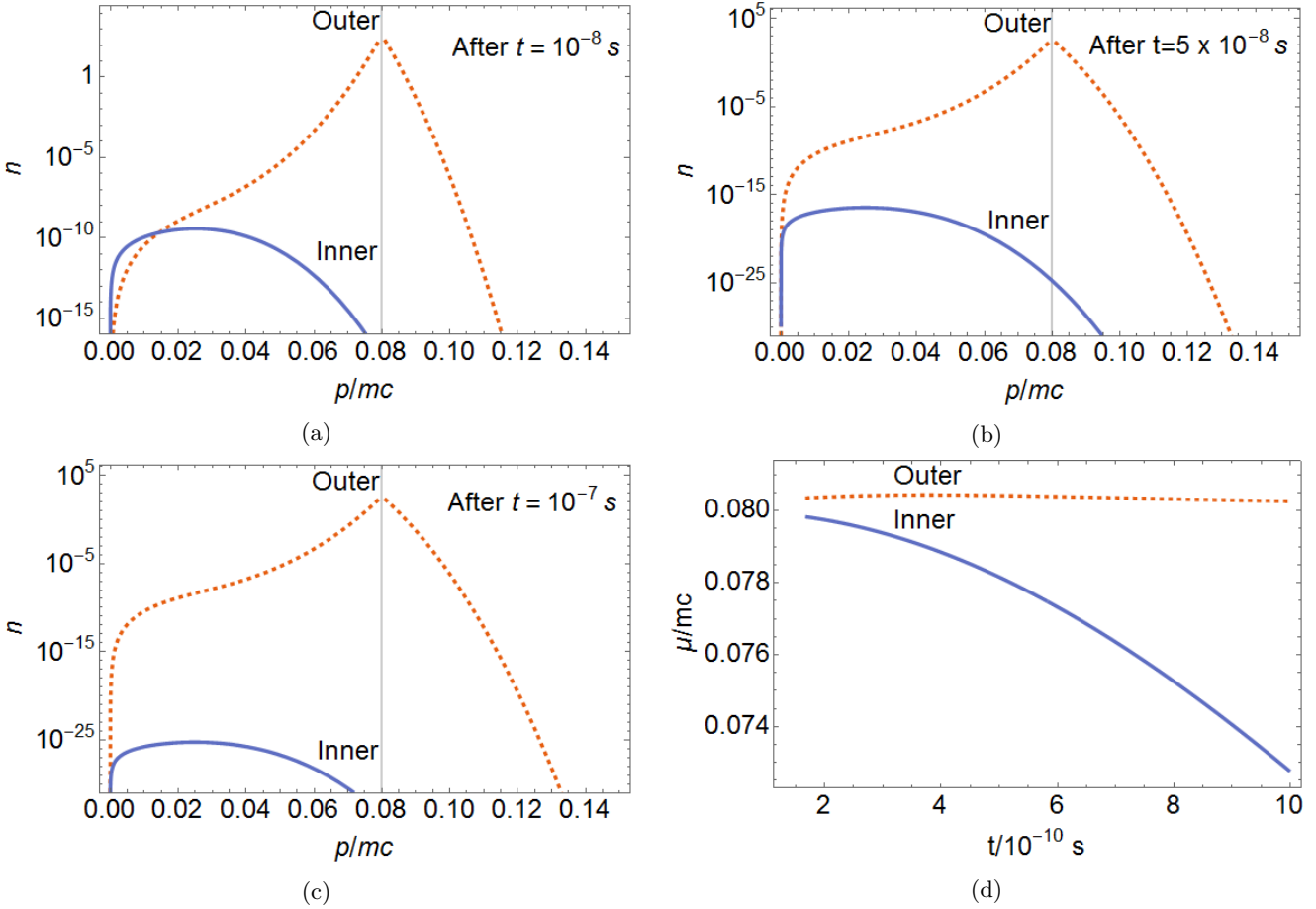


FIG. 1: The particle distribution functions inside (solid) and outside (dashed) the plasma. The vertical line indicates the initial proton momentum. The outer distribution does not change significantly after  $\sim 10^{-8}$  s (c.f. panels 1a-1c) while the inner distribution falls off quickly. Panel 1d shows the time dependence of the mean momentum.

which is larger than the predicted energy gain of  $\sim 0.01$  MeV. The expected width of the distribution is  $\Delta E_{\text{FWHM}} \sim 0.4$  MeV, i.e.  $\sim 15\%$  of the proton energy.

Applying the same approximations to the inner distribution, we find for the mean energy  $\mu_{\text{inner}} \sim 0.6$  MeV. This distribution, however, is not relevant any more, as the overall probability to find a particle inside the plasma after such long times has dropped to

$$N_{\text{inner}} = \int_0^1 n_{\text{inner}} d\hat{p} \sim 10^{-28}. \quad (27)$$

Here the upper limit was chosen such that it is much bigger than the mean initial momentum  $p_0$  and thus out of reach of the acceleration process.

Note that the numbers above correspond to impulsive injection of one particle ( $C_0 = 1$ ) at one point in time. Our result can be simply extended for multiple impulsive injections by appropriate superposition of the solution. If the time during which particles are injected is shorter than both the plasma and detector accumulation time, then the resultant proton spectrum is just that for a single impulsive injection scaled by a multiplicative factor.

We do the same analysis assuming a higher peak magnetic field of  $B \sim 3.6$  MG, which as noted before guarantees the system to be in the diffusive regime. As Fig. 2 shows, both the inner and outer distributions start off at the initial momentum for times around the escape time of these particles. Subsequently the mean momentum of the outer distribution increases due to the biased escape, and decreases only when the time is long enough for slower particles to escape the plasma.

As expected, the mean proton energy is now higher than before:  $\Delta\mu_e \sim 200$  keV. The same is true for the FWHM, which increases to:  $\Delta E_{\text{FWHM}} \sim 1.2$  MeV. This is consistent with the Hillas limit, which for the changed plasma parameters reads  $E_{\text{Hillas}} = 0.71$  MeV.

Finally, as mentioned earlier, we need to consider that the protons are not all injected with the same energy. However the thermal broadening is expected to be 30-40 keV [32] (see also Ref.[33]), i.e. an order of magnitude smaller than our calculated effect.

In ascribing any measured energy shift and spectral broadening to the 2nd-order Fermi mechanism, it must be noted that target charging, generation of static electric

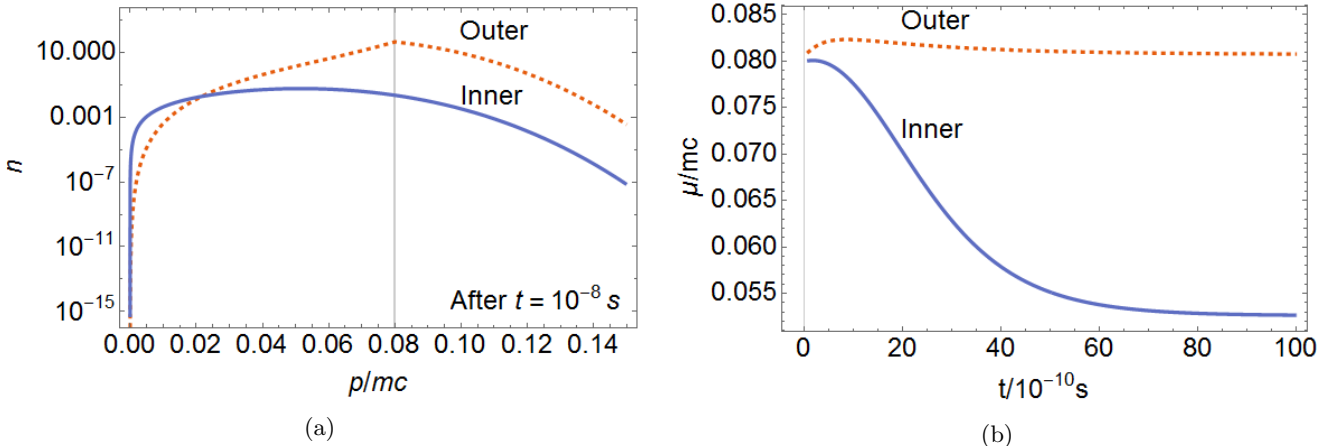


FIG. 2: The particle distribution functions inside (solid) and outside (dashed) the plasma taking  $B = 3.6$  MG. The vertical line indicates the initial proton momentum. Panel 2b shows the time dependence of the mean momentum.

fields due to the escape of hot electrons and energy loss by collisions can all obscure the signal [34, 35]. Other experiments with the proposed set-up are evaluating these effects and indicate that the resulting distortions are in fact negligible [36]. Therefore given plasma conditions as in Table I, and certainly for a 3 times stronger magnetic field, 2nd-order Fermi acceleration of D-D fusion protons should be measurable at the NIF.

To summarise, we have presented a suitable experimental set-up for measuring stochastic acceleration of protons in a turbulent plasma. If realised, this would

provide a platform where basic physical processes related to the classic Fermi theory of cosmic ray acceleration can be directly tested and validated against numerical simulations.

We would like to thank John Foster for valuable input. The research leading to these results has received funding from AWE plc. and the Engineering and Physical Sciences Research Council (grant numbers EP/M022331/1, EP/N014472/1 and EP/P010059/1). SS acknowledges a Niels Bohr Professorship awarded by the DNRF. ©British Crown Copyright 2018/AWE

---

[1] D. E. Hall and P. A. Sturrock. Diffusion, scattering, and acceleration of particles by stochastic electromagnetic fields. *The Physics of Fluids*, 10(12):2620, 1967.

[2] Russell M. Kulsrud. Important plasma problems in astrophysics. *Physics of Plasmas*, 2(5):1735, 1995.

[3] A. A. Schekochihin and S. C. Cowley. Turbulence, magnetic fields, and plasma physics in clusters of galaxies. *Physics of Plasmas*, 13(5):056501, 2006.

[4] A Marcowith, A Bret, A Bykov, M E Dieckman, L OC Drury, B Lembge, M Lemoine, G Morlino, G Murphy, G Pelletier, I Plotnikov, B Reville, M Riquelme, L Sironi, and A Stockem Novo. The microphysics of collisionless shock waves. *Reports on Progress in Physics*, 79(4):046901, 2016.

[5] G Gregori, B Reville, and F Miniati. The generation and amplification of intergalactic magnetic fields in analogue laboratory experiments with high power lasers. *Physics Reports*, 601:1–34, 2015.

[6] Enrico Fermi. On the origin of the cosmic radiation. *Phys. Rev.*, 75:1169–, 1949.

[7] E. Fermi. Galactic Magnetic Fields and the Origin of Cosmic Radiation. *The Astrophysical Journal*, 119:1, 1954.

[8] A. R. Bell. The acceleration of cosmic rays in shock fronts. I. *Monthly Notices of the Royal Astronomical Society*, 182:147, 1978.

[9] R. D. Blandford and J. P. Ostriker. Particle acceleration by astrophysical shocks. *Astrophysical Journal*, 221:L29, 1978.

[10] Roger Blandford and David Eichler. Particle acceleration at astrophysical shocks: A theory of cosmic ray origin. *Physics Reports*, 154(1):1, 1987.

[11] Vahé Petrosian. Stochastic acceleration by turbulence. *Space Science Reviews*, 173(1):535, 2012.

[12] R. Cowsik and S. Sarkar. The evolution of supernova remnants as radio sources. *Monthly Notices of the Royal Astronomical Society*, 207:745, 1984. Erratum: *ibid*, 209:719, 1984.

[13] G. J. Nelson and D. B. Melrose. *Type II bursts*, page 333. Cambridge University Press, 1985.

[14] Tramacere, A., Massaro, F., and Cavalieri, A. Signatures of synchrotron emission and of electron acceleration in the x-ray spectra of mrk 421. *A&A*, 466(2):521, 2007.

[15] S. O’Sullivan, B. Reville, and A. M. Taylor. Stochastic particle acceleration in the lobes of giant radio galaxies. *Monthly Notices of the Royal Astronomical Society*, 400(1):248, 2009.

[16] M. J. Hardcastle, C. C. Cheung, I. J. Feain, and . Stawarz. High-energy particle acceleration and production of ultra-high-energy cosmic rays in the giant lobes of centaurus a. *Monthly Notices of the Royal Astronomical Society*, 393(3):1041, 2009.

[17] P. Mertsch and S. Sarkar. Fermi Gamma-Ray “Bubbles”

from Stochastic Acceleration of Electrons. *Physical Review Letters*, 107(9):091101, 2011.

[18] P Tzeferacos, A Rigby, AFA Bott, AR Bell, R Bingham, A Casner, F Cattaneo, EM Churazov, J Emig, F Fiuzza, CB Forest, J Foster, C Graziani, J Katz, M Koenig, C.-K. Li, J Meinecke, R Petrasso, H.-S. Park, BA Remington, JS Ross, D Ryu, D Ryutov, TG White, B Reville, F Miniati, AA Schekochihin, DQ Lamb, DH Froula, and G Gregori. Laboratory evidence of dynamo amplification of magnetic fields in a turbulent plasma. *Nature Communications*, 9(1):591, 2018.

[19] W.J. Hogan, E.I. Moses, B.E. Warner, M.S. Sorem, and J.M. Soures. The national ignition facility. *Nuclear Fusion*, 41(5):567, 2001.

[20] J Meinecke, HW Doyle, F Miniati, AR Bell, R Bingham, R Crowston, RP Drake, M Fatenejad, M Koenig, Y Kuramitsu, CC Kuranz, DQ Lamb, D Lee, MJ MacDonald, CD Murphy, H-S. Park, A Pelka, A Ravasio, Y Sakawa, AA Schekochihin, A Scopatz, P Tzeferacos, WC Wan, NC Woolsey, R Yurchak, B Reville, and G Gregori. Turbulent amplification of magnetic fields in laboratory laser-produced shock waves. *Nature Physics*, 10(7):520–524, 2014.

[21] Jena Meinecke, Petros Tzeferacos, Anthony Bell, Robert Bingham, Robert Clarke, Eugene Churazov, Robert Crowston, Hugo Doyle, Paul R Drake, Robert Heathcote, Michel Koenig, Yasuhiro Kuramitsu, Carolyn Kuranz, Dongwook Lee, Michael MacDonald, Christopher Murphy, Margaret Notley, Hye-Sook Park, Alexander Pelka, Alessandra Ravasio, Brian Reville, Youichi Sakawa, Willow Wan, Nigel Woolsey, Roman Yurchak, Francesco Miniati, Alexander Schekochihin, Don Lamb, and Gianluca Gregori. Developed turbulence and nonlinear amplification of magnetic fields in laboratory and astrophysical plasmas. *Proceedings of the National Academy of Sciences*, 112(27):8211–8215, 2015.

[22] J. S. Ross, D. P. Higginson, D. Ryutov, F. Fiuzza, R. Hatarik, C. M. Huntington, D. H. Kalantar, A. Link, B. B. Pollock, B. A. Remington, H. G. Rinderknecht, G. F. Swadling, D. P. Turnbull, S. Weber, S. Wilks, D. H. Froula, M. J. Rosenberg, T. Morita, Y. Sakawa, H. Takabe, R. P. Drake, C. Kuranz, G. Gregori, J. Meinecke, M. C. Levy, M. Koenig, A. Spitkovsky, R. D. Petrasso, C. K. Li, H. Sio, B. Lahmann, A. B. Zylstra, and H.-S. Park. Transition from collisional to collisionless regimes in interpenetrating plasma flows on the national ignition facility. *Phys. Rev. Lett.*, 118:185003, 2017.

[23] B. Tverskoi. Contribution to the theory of fermi statistical acceleration. *JETP*, 25:317, 1967.

[24] M. Ostrowski and G. Siemieniec-Ozieblo. Diffusion in momentum space as a picture of second-order fermi acceleration. *Astroparticle Physics*, 6(3):271, 1997.

[25] S. A. Kaplan. The Theory of the Acceleration of Charged Particles by Isotropic Gas Magnetic Turbulent Fields. *Soviet Physics*, 2:203, 1956.

[26] Philipp Mertsch. A new analytic solution for 2nd-order fermi acceleration. *Journal of Cosmology and Astroparticle Physics*, 2011(12):010, 2011.

[27] V. Rozhansky and O.G. Bakunin. *Reviews of Plasma Physics*. Number 24. Springer Berlin Heidelberg, 2008.

[28] T.R Boehly, D.L Brown, R.S Craxton, R.L Keck, J.P Knauer, J.H Kelly, T.J Kessler, S.A Kumpan, S.J Loucks, S.A Letzring, F.J Marshall, R.L McCrory, S.F.B Morse, W Seka, J.M Soures, and C.P Verdon. Initial performance results of the omega laser system. *Optics Communications*, 133(1):495 – 506, 1997.

[29] N. S. Kardashev. Nonstationarity of Spectra of Young Sources of Nonthermal Radio Emission. *Soviet Astronomy*, 6:317, 1962.

[30] Peter A. Becker, Truong Le, and Charles D. Dermer. Time-dependent stochastic particle acceleration in astrophysical plasmas: Exact solutions including momentum-dependent escape. *The Astrophysical Journal*, 647(1):539, 2006.

[31] A. M. Hillas. The origin of ultra-high-energy cosmic rays. *Annual Review of Astronomy and Astrophysics*, 22(1):425, 1984.

[32] L. Ballabio, J. Kllne, and G. Gorini. Relativistic calculation of fusion product spectra for thermonuclear plasmas. *Nuclear Fusion*, 38(11):1723, 1998.

[33] G. Lehner and F. Pohl. Reaktionsneutronen als hilfsmittel der plasmadiagnostik. *Zeitschrift für Physik*, 207(1):83, 1967.

[34] A. B. Zylstra, J. A. Frenje, P. E. Grabowski, C. K. Li, G. W. Collins, P. Fitzsimmons, S. Glenzer, F. Graziani, S. B. Hansen, S. X. Hu, M. Gatup Johnson, P. Keiter, H. Reynolds, J. R. Rygg, F. H. Séguin, and R. D. Petrasso. Measurement of charged-particle stopping in warm dense plasma. *Phys. Rev. Lett.*, 114:215002, 2015.

[35] D. G. Hicks, C. K. Li, F. H. Sguin, A. K. Ram, J. A. Frenje, R. D. Petrasso, J. M. Soures, V. Yu. Glebov, D. D. Meyerhofer, S. Roberts, C. Sorce, C. Stckl, T. C. Sangster, and T. W. Phillips. Charged-particle acceleration and energy loss in laser-produced plasmas. *Physics of Plasmas*, 7(12):5106, 2000.

[36] L. E. Chen, A. F. A. Bott, P. Tzeferacos, A. Rigby, A. Bell, R. Bingham, C. Graziani, J. Katz, M. Koenig, C. K. Li, R. Petrasso, H.-S. Park, J. S. Ross, D. Ryu, D. Ryutov, T. G. White, B. Reville, J. Matthews<sup>1</sup>, J. Meinecke, F. Miniati, E. G. Zweibel, S. Sarkar, A. A. Schekochihin, D. Q. Lamb, D. H. Froula, and G. Gregori. Analogue of cosmic ray transport in a laboratory turbulent plasma. in preparation, 2018.